Paper Physics
TAPPI FOUNDATION

Micro-model of paper

Part 2: Statistical analysis of the paper structure

Wentao Lu and Leif A. Carlsson

ABSTRACT: Part 2 describes the Monte Carlo simulation of the formation and microstructure of paper to obtain volume fractions of bonds and fiber segments. A paper sheet is considered as a two-dimensional planar structure formed by initially straight fibers of uniform length, width, and thickness. The position and the orientation of each fiber in the sheet are generated by the Monte Carlo method. Averages of certain geometrical structural parameters are calculated and expressed in terms of apparent sheet density.

KEYWORDS: Bonded area, fiber length, fiber orientation, formation, geometry, mathematical models, microstructure, paper sheets, paper structure, simulation, voids.

Our main objective in this study is to develop a simulation model for the formation of isotropic and oriented papers of any given apparent density. Microstructural details such as fiber crossings, free segments, and voids govern the mechanical properties of paper *(1–4)*. Consequently, for modeling purposes, the volume fractions of bonds, free segments, and voids have to be determined.

In Part 1, we considered bonded regions as assemblages of cell-wall elements connected in parallel and free segments as cell-wall elements connected in series *(5)*. Here, we present the Monte Carlo simulation of sheet formation and structure. This technique is used to calculate the additional parameters of paper microstructure needed in Part 3 to predict the elastic and hygroexpansion properties of paper.

Background

To directly measure the number of fiber-to-fiber contacts in a sheet of paper is virtually impossible because of the small dimensions of the fibers and bonds and the intractable structure of the paper. The description of the geometrical structure of paper is further complicated by the variations in dimensions, shapes, and orientations of the fibers. Moreover, a significant fraction of the volume is taken up by voids of various geometries and sizes.

Lu is a graduate student and Carlsson is a professor at the Department of Mechanical Engineering, Florida Atlantic University, Boca Raton, FL 33431.

The complexity of the microstructure of paper makes it necessary to take a statistical approach to the geometrical analysis. Efforts have been made to calculate the structural parameters from more accessible parameters such as fiber orientation and fiber length. Van Wyk considered paper as a random assembly of uniform cylindrical fibers and derived an expression for the average distance between contact points *(6)*. Corte and Kallmes studied the geometry of paper and recognized that since no fibers traverse the thickness of the sheet, the structure may be considered as approximately two-dimensional *(7, 8)*. They simulated paper with straight-line segments all of the same length, with each segment placed at a random location at a random planar angle. By this approach, several structural properties of paper were derived analytically.

Komori and Makishima later introduced an alternative method for calculating the number of fiber-to-fiber contacts in a fiber assemblage of a certain volume *(9)*. Their analysis includes oriented fiber assemblages and is not limited to planar random networks. Van den Akker identified the total bonded area in a sheet of paper as an important structural parameter governing the mechanical properties of paper and derived expressions for its calculation *(3)*. Perkins later suggested alternative statistical methods for calculating the bonded area *(4)*.

As Corte pointed out, the structural description of paper could start

1. A fiber of dimensions L_{fiber} x W_{fiber} x T_{fiber} is deposited at left into an area *a* x *a*. On the right, the region covered by the fiber is subdivided into small square areas, or elements.

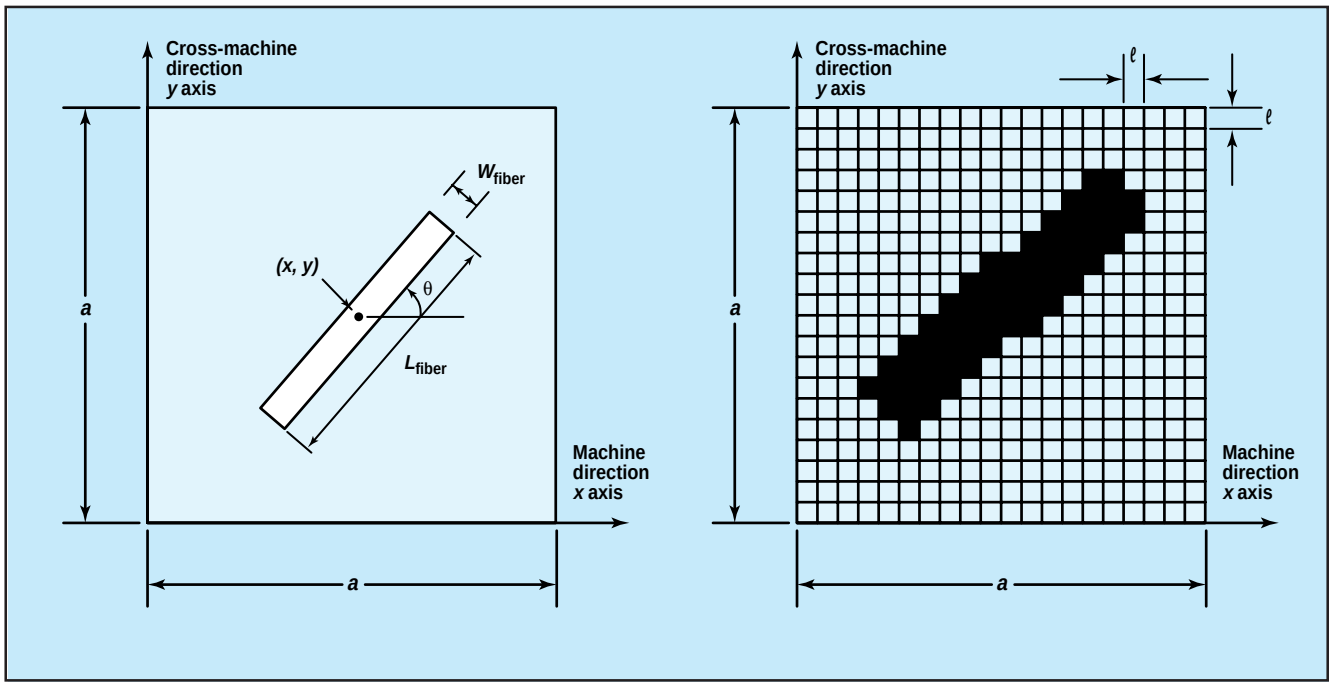

with an analysis of a simulated thin paper network constructed of random line segments *(7)*. We have adopted this approach in the work presented here. A computer-aided Monte Carlo simulation is performed to describe the formation and structure of a paper sheet. Microstructural parameters such as the number of fiber-to-fiber contacts (bonds), the bonded area, the average segment length, and volume fractions of fiber segments and bonds are calculated and expressed in terms of apparent sheet density.

Monte Carlo simulation of paper formation

The Monte Carlo method *(10)* provides a solution to certain mathematical problems through the simulation of the outcome of a process using random numbers. The simulation process is repeated several times, each trial being independent of the previous. The average of the process can be obtained with an accuracy and a precision that increase with the number of trials.

Certain microstructural characteristics of the paper structure are calculated based on a Monte Carlo simulation of the formation and structure of paper. These characteristics include the number of fiber crossings (bonds), the total bonded area, the average length of free fiber segments, and the volume fractions of bonds, free segments, and voids. Because the fibrous structure of paper is extremely complex, many simplifications and assumptions are necessary.

Selecting a representative area

First, consider paper as a two-dimensional planar structure. The simulation of the sheet-forming process starts with the selection of a representative area of the paper sheet. It is possible to base the simulation on actual sheet and fiber dimensions, or a different scale for length may be used. If a different scale is used, all linear dimensions should be scaled similarly.

In this study, our procedure was to select a square region of side length *a*, where *a* should be much larger than the fiber width. **Figure 1** shows these dimensions in the graph on the left. The fibers are assumed to be band-shaped, straight, and of uniform length L_{fiber}, width W_{fiber}, and thickness T_{fiber}. In the graph on the right, the region is subdivided into small square areas, or elements. Each element has a side length equal to a/M, where M is the number of divisions of the side length. Each element is represented by the coordinates of its midpoint.

A fiber with position coordinates and orientation angle generated by the Monte Carlo method is placed in the region. Depending on the position, orientation, and dimensions of the fiber, certain elements will be activated, as indicated by the small filled squares in Fig. 1. The region occupied by a fiber is represented in this way by a set of coordinates for the centers of the activated elements. An accurate numerical representation of the region occupied by the fiber can be obtained by selecting a large number of small divisions of the area (i.e., small elements).

2. Simulated paper sheets consisting of 100 fibers, one moderately oriented (left) and one highly oriented (right).

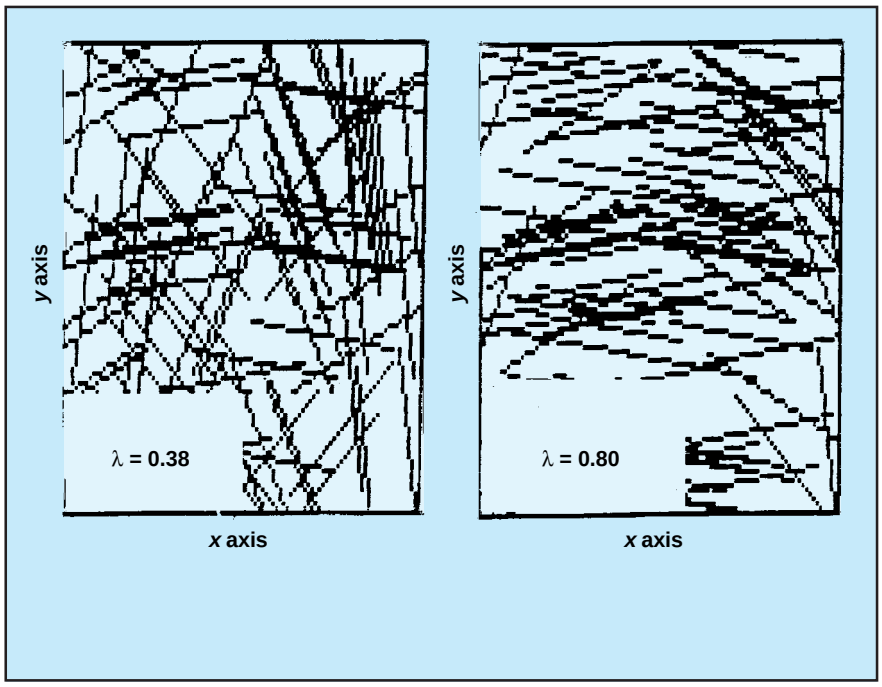

The position coordinates of the center of a fiber (*x*,*y* in Fig. 1) are random variables generated by the pseudo-random number method *(10)*. By this process, we obtain a uniform distribution of positions of the fibers. The fiber orientation is defined by the angle between the fiber axis and the *x* axis. In general, the fibers are not uniformly oriented. In the Monte Carlo simulation, the angle is weighted by the fiber orientation distribution function *(11)*, defined by the wrapped Cauchy distribution *(12)*:

$$f(\theta) = (1/\pi)\,[(1-\lambda^2)/(1+\lambda^2-2\lambda\cos 2\theta)] \quad (1)$$

where λ is the orientation parameter ($0 \le \lambda \le 1$). For isotropy, λ is equal to 0. For perfect collimation of the fibers, λ is equal to 1.

Figure 2 shows examples of two simulated paper sheets, one moderately oriented (λ = 0.38) and one highly oriented (λ = 0.80). Each consists of 100 fibers of dimensions L_{fiber} = 1 mm, W_{fiber} = 25 μm, and T_{fiber} = 5 μm. The saw-tooth appearance of the fibers is caused by the limited resolution of the computer screen and does not influence the accuracy of the simulations. As easily visualized, the fibers become more aligned with the machine direction when the orientation distribution narrows as λ increases.

Segment length and bonded area

A fiber crossing, or "bond," is the region of contact between two adjacent fibers. A free fiber segment is the region of the fiber having no contact with any other fibers—that is, the region between the bonds. **Figure 3** illustrates these definitions.

Mathematically a bond is defined to occur only when the axes of two fibers cross each other, although it is recognized that two fibers may partially overlap, as shown in **Fig. 4A**. The fibers are represented by straight line segments, and the bonded regions collapse to points at the fiber crossing sites, as shown in **Fig. 4B**.

In forming the simulated sheet, it is possible to identify the contact region between previously deposited fibers and each newly deposited fiber. Each newly deposited fiber is assumed to be flexible enough to bond to the fibers underneath, as **Fig. 5** illustrates. If more than two fibers are crossing at one "point" (i.e., within a small area), this condition corresponds to a multiple bond.

The average number of fiber crossings, χ_{fiber}, on an arbitrary fiber (of length L_{fiber}) can be obtained by Eq. 2 *(7)*:

$$\chi_{fiber} = 2\chi/N \quad (2)$$

where χ is the total number of fiber crossings and N is the number of deposited fibers. The factor 2 in Eq. 2 is introduced to account for the fact that fiber-to-fiber bonds appear on opposite sides of the fiber. The average length between two adjacent fiber crossings, or the length of the free fiber segment, is

$$L_{seg} = (N\,L_{fiber})/(2\chi) \quad (3)$$

The bonded area formed between a fiber being placed and the fibers previously placed is approximated by the area of overlapping elements, as defined in Fig. 1. After all fibers are placed, the total fiber–fiber bonded area, A_{TB}, which is the sum of areas between any two bonded fibers for the entire sheet, is

$$A_{TB} = N_{TB}\,\ell^2 \quad (4)$$

where N_{TB} is the total number of bonded areas (ℓ x ℓ) between any two fibers. The average bonded area for each bond site, A_{bond}, can be calculated by dividing A_{TB} by the number of fiber crossings, χ:

$$A_{bond} = A_{TB}/\chi \quad (5)$$

Volume fractions of free fiber segments and bonds

To obtain the volume fractions of free fiber segments and bonded material, we calculate the number of elements occupied by free fiber segments and bonds, N_{segs} and N_{bonds}. Since each elemental area is of dimensions ℓ x ℓ, the total areas occupied by free fiber segments and bonds are $N_{segs}\,\ell^2$ and

3. A free fiber segment is a section of fiber free of contact with another fiber, and bonded areas are places where fibers cross.

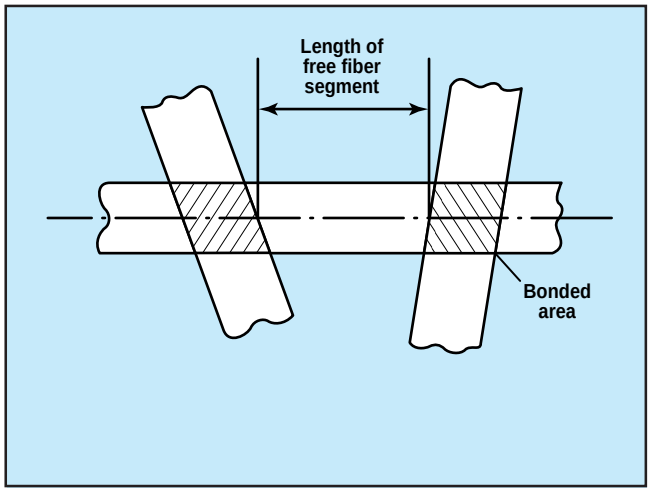

4. Bonded regions showing (A) fibers of width W_{fiber} and (B) the same fibers represented as having no width

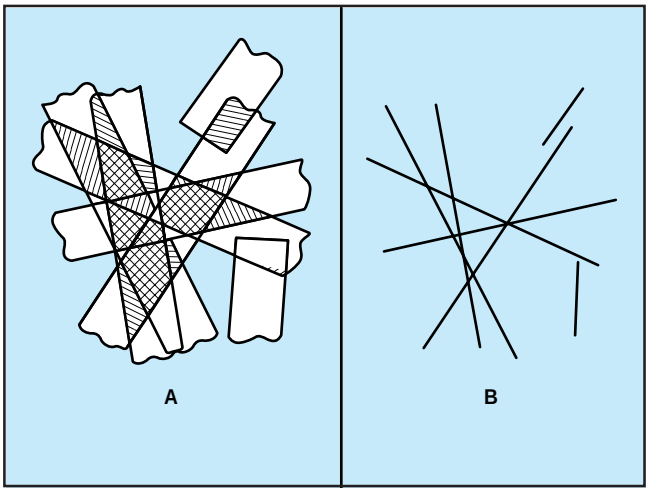

$N_{bonds}\ \ell^2$, respectively. Each free fiber segment has the thickness of a fiber, and thus the total volume of free fiber segments is $N_{segs}\ \ell^2\ T_{fiber}$.

At each bond site, several fibers may overlap, as Fig. 4A shows. The total thickness of a bonded region is the sum of the overlapping fiber thicknesses. Rather than calculate each bond volume, we base the calculation of total bond volume on the average bond thickness, $<T_{bond}>$. This average thickness is obtained by averaging the thicknesses of all bonded regions. The total volume of the bonded regions is thus equal to $N_{bonds}\ \ell^2\ <T_{bond}>$. The thickness, T, of the simulated sheet is defined as the average bond thickness. The volume fractions of free fiber segments and bonded material, V_{segs}, and V_{bonds} are then

$$V_{segs} = (N_{segs}\ \ell^2\ T_{fiber})/(A\ T) \qquad (6a)$$

$$V_{bonds} = (N_{bonds}\ \ell^2\ <T_{bond}>)/(A\ T) = (N_{bonds}\ \ell^2)/A \qquad (6b)$$

where $A = a^2$ and ℓ is defined in Fig. 1. The volume fraction of voids, V_{voids}, is simply given by

$$V_{voids} = 1 - (V_{segs} + V_{bonds}) \qquad (7)$$

The apparent sheet density, ρ_{sheet}, is given by the total mass of deposited fibers over the area A divided by the sheet volume, A x T:

$$\rho_{sheet} = (N\ L_{fiber}\ W_{fiber}\ T_{fiber}\ \rho_{cw})/(A\ T) \qquad (8)$$

where ρ_{cw} is the density of the cell wall (ρ_{cw} = 1500 kg/m^3) *(13)*. As an alternative, ρ_{sheet} can be calculated from the void content using the following equation *(14)*:

$$\rho_{sheet} = \rho_{cw}\ (1 - V_{voids}) \qquad (9)$$

I. Number of fiber crossings, χ, and normalized thickness of simulated paper sheets, T_{normal}, for fibers deposited in numbers ranging from 10 to 300.

	Fiber crossings, χ, for numbers of fibers						
λ	*10*	*50*	*100*	*150*	*200*	*250*	*300*
0.01	6	89	334	709	1223	1808	2534
0.11	5	88	331	697	1215	1768	2494
0.38	4	90	316	679	1082	1668	2300
0.50	5	81	299	640	1038	1560	2170
0.80	2	49	201	403	672	1050	1480
0.95	1	29	132	262	466	754	1035
T_{normal}	2.00	2.03	2.12	2.21	2.23	2.33	2.41

L_{fiber} = 1 mm. W_{fiber} = 30 µm. T_{fiber} = 5 µm. T_{normal}=T/T_{fiber}.

Results and discussion

Using this approach, we simulated the formation of square sheets, 2.5 mm x 2.5 mm, with the number of fibers ranging from 10 to 300. The number, M, of divisions of the length a was 100. We considered fibers of the following dimensions: length L_{fiber} = 1, 2, and 3 mm; width W_{fiber} = 16, 25, and 50 µm; and thickness T_{fiber} = 5 µm. The values for the orientation parameter λ in the wrapped Cauchy distribution (Eq. 1) ranged from 0 to 0.95.

Number of fiber crossings

Table I lists the number of fiber crossings, χ, for specific values of λ and specific numbers of fibers deposited. As the table shows, the number of crossings increases as the number of fibers increases. The number of fiber crossings decreases with

II. Number of fiber crossings calculated from the analysis of Komori and Makishima (*9*)

	Fiber crossings for number of fibers deposited						
λ	10	50	100	150	200	250	300
0.01	5	127	510	1147	2038	3185	4586
0.11	5	126	505	1136	2019	3155	4543
0.38	5	115	458	1031	1834	2865	4126
0.50	4	105	420	945	1680	2625	3780
0.80	3	63	252	567	1008	1575	2268
0.95	1	24	96	216	384	600	864

L_{fiber} = 1 mm. W_{fiber} = 30 μm. T_{fiber} = 5 μm.

III. Total bonded area, A_{TB}

	Total bonded area, x 10^{-3} mm^2						
λ	10	50	100	150	200	250	300
0.01	6	113	431	964	1468	2423	3218
0.11	5	114	457	941	1470	2404	3242
0.38	5	116	420	978	1515	2402	3289
0.50	6	134	311	992	1588	2480	3385
0.80	4	110	519	1128	1808	2804	3759
0.95	1	97	585	1200	1831	2903	3954

L_{fiber} = 1 mm. W_{fiber} = 30 μm. T_{fiber} = 5 μm.

5. Fibers are assumed to be flexible enough to bond to the fibers underneath the first fibers they contact

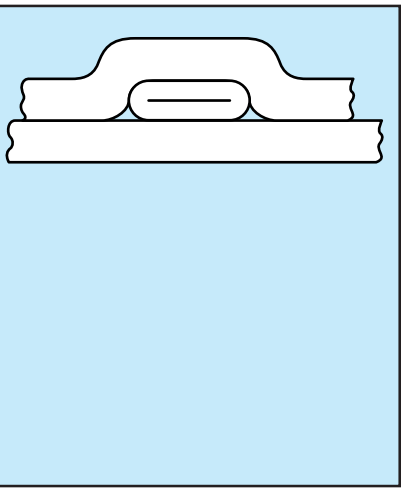

increased fiber alignment, or as λ increases. Furthermore, the sheet thickness increases with the number of fibers deposited. The fiber orientation has virtually no influence on the sheet thickness *(11)*, a result not shown in these tables.

Table II lists the results for the number of fiber crossings calculated from the analysis of Komori and Makishima *(9)*. These results tend to exceed the results from the Monte Carlo simulation in Table I, except for highly oriented fibers (λ → 1). Komori and Makishima actually calculated the *maximum* possible number of fiber crossings, because they confined the sheet volume to only two layers of fibers. As Table I shows, the simulated sheet thickness exceeds twice the fiber thickness when more than ten fibers are deposited. This means that there are more than two fiber layers, which reduces the frequency of fiber-to-fiber contacts and the number of bonds.

The total bonded area A_{TB} as defined by Eq. 4 is listed in **Table III.** A_{TB} increases with increasing numbers of fibers. For a reasonably large number of fibers, an increase in fiber orientation tends to increase the bonded area, although the number of fiber crossings decreases (as shown in Table I).

The average bonded area per bond site A_{Bond} (Eq. 5) increases with increasing fiber orientation, as **Table IV** shows. As the fiber alignment increases, the overlapping area increases along with the decrease in crossing angles. Evidently, this increase in overlapping area accounts for the increase in the average bonded area per bond site. Notice that for a given fiber orientation, A_{Bond} shows relatively small variations as the number of fibers in the sheet increases.

The results calculated from the analysis of Perkins *(4)* are also listed in Table IV. The agreement with the values derived from his analysis is reasonably good, except for very highly oriented fiber sheets. It is believed that Perkins's analysis overestimates A_{Bond} for sheets with highly oriented fibers (λ → 1) *(11)*.

The average number of fiber crossings on a fiber, χ_{fiber}, is calculated from Eq. 2. **Table V** shows that χ_{fiber} increases with the number of deposited fibers and decreases with increasing fiber orientation. Notice that for a small number of highly aligned fibers, not all the fibers are connected (χ_{fiber} < 1).

Table VI shows that the average segment length decreases with an increasing number of fibers and increases with an increasing degree of fiber orientation. A sheet with ran-

domly oriented fibers ($\lambda = 0$) has the largest average number of fiber crossings per fiber and has the smallest segment length. Table VI shows that for a small number of fibers *(10)*, a sheet has not formed: the average segment length exceeds the fiber length (1 mm), which is anomalous.

Volume fractions of segments and bonds

The volume fractions of free fiber segments and bonds, V_{segs} and V_{bonds}, were calculated from Eq. 6 for various fiber orientations (λ = 0, 0.38, and 0.80), fiber lengths (L_{fiber} = 1, 2, and 3 mm), and fiber widths (W_{fiber} = 16, 25, and 50 μm). **Figure 6** displays V_{bonds} and V_{segs} versus apparent sheet density ρ_{sheet} for various values of λ, L_{fiber}, and W_{fiber}.

The volume fractions of segments and bonds are not substantially influenced by the degree of fiber alignment (Fig. 6A). V_{bonds} increases with increased apparent sheet density, while V_{segs} goes through a maximum at $\rho_{sheet} \approx 500$ kg/m^3. Above this density, bonds occupy most of the solids volume of paper. For sheets with low apparent densities, free fiber segments are expected to dominate the response of the paper sheet. The insensitivities of V_{segs} and V_{bonds} to the fiber orientation parameter are evidently attributable to the combination of the increased area per bond site and the decreased number of bonds with increased fiber orientation (Tables I and II).

The curves for different fiber lengths almost coincide, as Fig. 6B shows. The fiber length thus has very little influence on the volume fractions at a given apparent sheet density. Similarly, the fiber width has only a slight influence on the volume fractions, as Fig. 6C shows.

Based on the Monte Carlo simulations and analysis presented here, the volume fractions V_{segs} and V_{bonds} are uniquely determined by the apparent sheet density.

IV. Average bonded area per bond site, A_{Bond}

	Average bonded area per bond site, x 10^{-3} mm^2							
λ	10	50	100	150	200	250	300	Perkins (4)
0.01	1.05	1.27	1.29	1.36	1.20	1.34	1.27	1.41
0.11	0.90	1.30	1.38	1.35	1.21	1.36	1.30	1.43
0.38	1.13	1.29	1.33	1.44	1.40	1.44	1.43	1.57
0.50	1.26	1.65	1.36	1.55	1.53	1.59	1.56	1.71
0.80	1.80	2.24	2.58	2.80	2.69	2.67	2.54	2.86
0.95	0.90	3.34	4.43	4.58	3.93	3.85	3.82	7.50

L_{fiber} = 1 mm. W_{fiber} = 30 μm. T_{fiber} = 5 μm.

V. Average number of fiber crossings on a fiber, χ_{fiber}

	Average number of fiber crossings per fiber						
λ	10	50	100	150	200	250	300
0.01	1.20	3.56	6.68	9.45	12.2	14.5	16.9
0.11	1.00	3.52	6.62	9.29	12.2	14.1	16.6
0.38	0.80	3.60	6.32	9.05	10.8	13.3	15.3
0.50	1.00	3.24	5.98	8.53	10.4	12.5	14.5
0.80	0.40	1.96	4.02	5.37	6.7	8.4	9.9
0.95	0.02	1.16	2.64	3.49	4.7	6.0	6.9

L_{fiber} = 1 mm. W_{fiber} = 30 μm. T_{fiber} = 5 μm.

VI. Average length of free fiber segments

	Average segment length, mm						
λ	10	50	100	150	200	250	300
0.01	0.75	0.24	0.12	0.089	0.067	0.058	0.048
0.11	0.88	0.24	0.12	0.090	0.067	0.059	0.049
0.38	1.06	0.23	0.13	0.092	0.076	0.063	0.054
0.50	0.87	0.26	0.14	0.100	0.081	0.068	0.058
0.80	2.34	0.47	0.23	0.168	0.133	0.107	0.090
0.95	4.74	0.81	0.35	0.260	0.195	0.151	0.132

L_{fiber} = 1 mm. W_{fiber} = 30 μm. T_{fiber} = 5 μm.

6. Volume fractions of bonds and free segments (V_{bonds} and V_{segs}) versus apparent sheet density, showing (A) the influence of fiber orientation, (B) the influence of fiber length, and (C) the influence of fiber width.

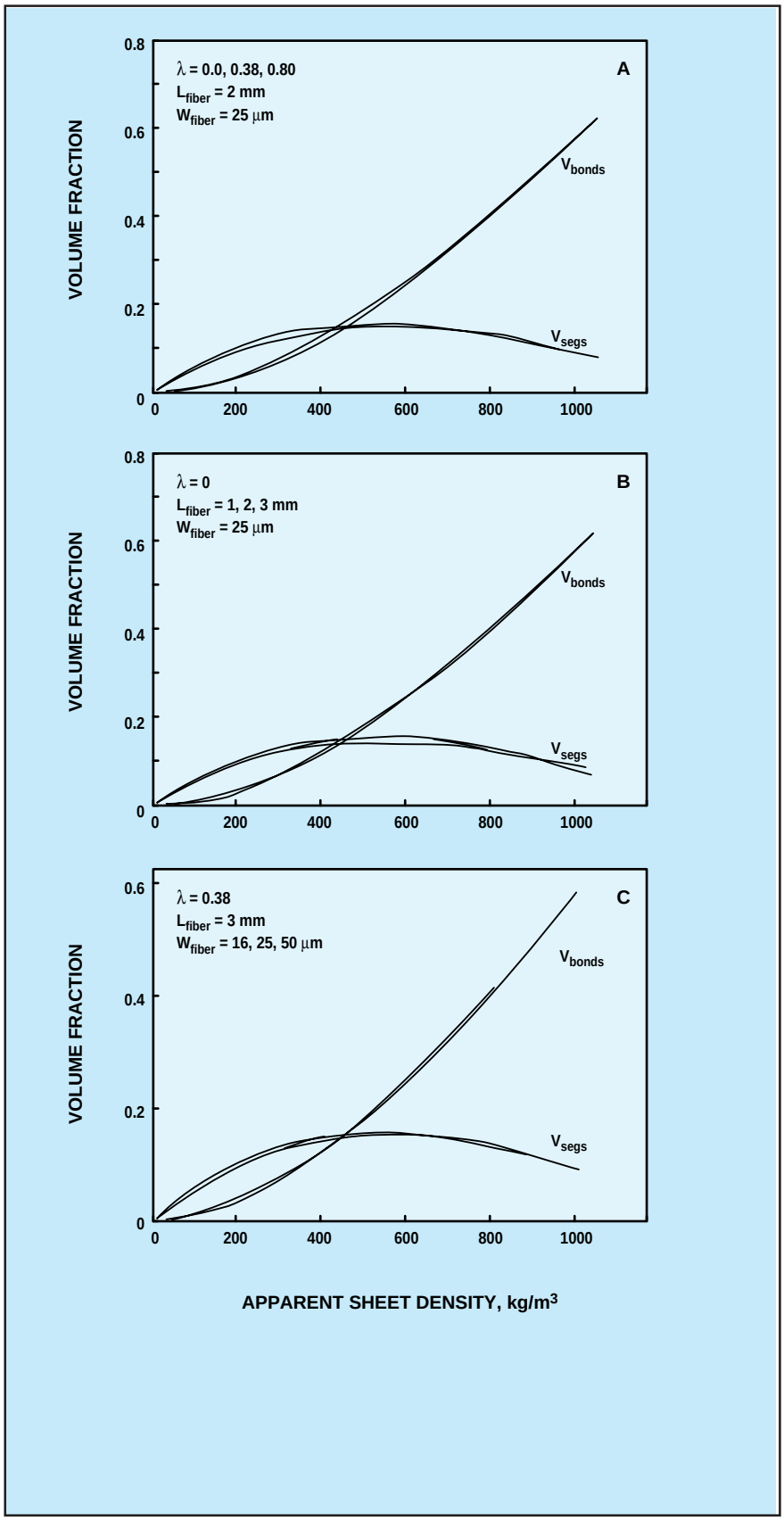

These results are based on the assumption that the fibers are flexible, which may be reasonable for collapsed chemical pulp fibers in a water-saturated state during sheet formation. However, the assumption may be less realistic for mechanical pulp fibers, which are stiffer.

Furthermore, the calculations were performed by subdividing the region into a finite number of elements. The numerical calculations are thus associated with discretization error, but the relatively small elements used lead to results for the average bonded area per bond site that closely agree with analytical predictions. Therefore, the predictions of the volume fractions are expected to be reasonable.

Conclusions

In Part 1, we derived elastic constants and moisture expansion coefficients. In Part 2, we have simulated sheet formation and have statistically analyzed the paper structure. To generate structural data required for making predictions with the micro model (Part 3), we used the Monte Carlo technique to simulate random and oriented paper sheets.

The results were compared with previously reported analytical predictions. The values calculated from the simulation for the average bonded area per bond site are very close to the analytical results, with the exception of the highly oriented sheets.

The trends of the number of fiber crossings versus the number of deposited fibers and fiber orientation are in qualitative agreement with the analytical predictions. However, the analytical procedure predicts more crossings than we found because the volume of the formed sheet in the analytical prediction is confined to two layers of fibers.

The volume fractions of bonds and segments in the simulated sheets were calculated for various values of the fiber orientation parameter and various lengths and widths of the

fibers. The volume fractions of bonds and segments at a given apparent sheet density were found to be affected very little by fiber orientation and fiber length and width. The apparent sheet density thus serves as a normalizing factor for the volume fractions of bonds and segments. TJ

Literature cited

1. Perkins, R. W. and Mark, R. E., *Tappi* 59(12): 18(1976).
2. Page, D. H. and Seth, R. S., *Tappi* 62(9): 99(1979); 63(6): 113(1980); 63(10): 99 (1980).
3. Van den Akker, J. A., in *Formation and Structure of Paper* (F. Bolam, Ed.), Tech. Sect. Brit. Paper and Board Makers Assn., London, 1962, Vol. I, p. 205.
4. Perkins, R. W., in *The Cutting Edge*, proceedings of the 1980 Conference of Paper Science and Technology, The Institute of Paper Chemistry, Appleton (now The Institute of Paper Science and Technology, Altanta), 1980, p. 89.
5. Lu, W., Carlsson, L. A., and Andersson, A., *Tappi J.* 78(12):(1995).
6. Van Wyk, C. M., *J. Textile Inst.* 37: T285(1946).
7. Corte, H., in *Structure, Solid Mechanics and Engineering Design*, proceedings of the Southampton 1969 Civil Engineering Conference, Wiley Interscience, 1971, p. 341.
8. Kallmes, O. and Corte, H., *Tappi* 43(9): 737(1960).
9. Komori, T. and Makishima, K., *Textile Research J.* 47: 1(1977).
10. Sobol´, I. M., *The Monte Carlo Method*, The University of Chicago Press, Chicago, 1974.
11. Lu, W., "Micro-model for paper," M.S. thesis, Dept. of Mechanical Engineering, Florida Atlantic University, Boca Raton, FL, August 1994.
12. Shulgasser, K., *J. Mater. Sci.* 20: 859(1985).
13. Salmen, L., Carlsson, L., de Ruvo, A., Fellers, C., and Htun, M., *Fibre Sci. Technol.* 20: 283(1984).
14. Bristow, J. A., "The Pore Structure and Sorption of Liquids," in *Paper Structure and Properties* (J. A. Bristow and P. Kolseth, Eds.), Marcel Dekker, New York, 1986, p. 183.

The authors are grateful for financial support provided by the TAPPI Foundation (Pe-96-93).

Received for review Nov. 20, 1994.

Accepted May 10, 1995.

Research for this paper was supported through funding by the TAPPI Foundation. For information on the Foundation, call (770) 446-1400. ext. 266 or 211. Information is also available on the TAPPI Web site in the "About TAPPI" section. The address is http://www.tappi.org.